Short communication

Core/shell magnetic mesoporous silica nanoparticles with radially oriented wide mesopores

Nikola Ž. Knežević[*]

Faculty of Pharmacy, European University, Trg mladenaca 5, 21000 Novi Sad, Serbia

Abstract

Core/shell nanoparticles, containing magnetic iron-oxide (maghemite) core and mesoporous shell with radial porous structure, were prepared by dispersing magnetite nanoparticles and adding tetraethylorthosilicate to a basic aqueous solution containing structure-templating cetyltrimethylammonium bromide and a pore-swelling mesithylene. The material is characterized by SEM and TEM imaging, nitrogen sorption and powder X-ray diffraction. Distinctive features of the prepared material are its high surface area (959 m^2/g), wide average pore diameter (12.4 nm) and large pore volume (2.3 cm^3/g). The material exhibits radial pore structure and the high angle XRD pattern characteristic for maghemite nanoparticles, which are obtained upon calcination of the magnetite-containing material. The observed properties of the prepared material may render the material applicable in separation, drug delivery, sensing and heterogeneous catalysis.

Keywords: nanofabrication, core/shell structure, maghemite, mesoporous silica, large mesopores

I. Introduction

Mesoporous silica nanomaterials (MSN) have attracted much attention in recent years owing to their large surface area (up to 1000 m^2/g), tunable pore diameter (2–50 nm), narrow pore size distribution, and high thermal stability. The material has been demonstrated as applicable for selective catalysis [1–3], drug delivery [4–6], sensing [7] and separation techniques [8–10].

Magnetic analogues of mesoporous silica nanoparticles (MMSN), which would contain the same beneficial characteristics of non-magnetic material, but with an added feature of being responsive to magnetic field, are of particular interest [11]. Hence, all of the above mentioned applications of the materials can be improved, as drug delivery systems would be capable of magnetic field-guided therapy and magnetic resonance imaging [12,13], or the material would be easily removed by magnetic field after performing its catalytic, sensing or separating function.

Various synthetic pathways have been implemented to obtain magnetic materials with different core/shell structures. Authors reported MMSN material with irregular [14,15], radial [16] and hexagonal pore ordering [17,18]. We previously synthesized superparamagnetic MMSN materials with high surface areas, which contain radial and hexagonal porous structures, for application in drug delivery to cancer cells [19,20]. Herein we communicate on synthesis and characterization of wide pore MMSN material (WPMMSN), with radial porous structure, as inspired by the previously reported wide pore MSN material [21], which was capable of storing and delivering enzymes into cancer cells.

II. Experimental

All chemicals used for the preparation of the materials were purchased (Aldrich) and used as received. Magnetite nanoparticles were prepared as previously reported [20,22] by co-precipitation of Fe^{3+} and Fe^{2+} ions with NH_4OH in aqueous solution. The obtained magnetite nanoparticles (80 mg) were sonicated for 12 h in 10 mL of nanopure water and added dropwise into a solution containing n-cetyltrimethylammonium bromide (CTAB) (1 g, 2.7 mmol), mesithylene (7 mL, 0.05 mol) and NaOH (3.5 ml, 2M) in 480.0 ml of water. The suspension was then stirred with mechanical stirrer and

---

[*] Corresponding author: tel: +381 21 6615 897
e-mail: *nikola.z.knezevic@gmail.com*

heated to 80 °C before dropwise addition of 5.0 ml of tetraethylorthosilicate TEOS (22.4 mmol). After additional stirring for 2 h at 80 °C, as-synthesized light-brown material was filtrated, washed with water and methanol and air dried. Final WPMMSN was obtained upon removal of surfactant under calcination at 550 °C for 6 h with a heating rate of 10 °C/min.

Powder XRD diffraction data were collected on a Scintag XRD 2000 X-ray diffractometer using Cu Kα radiation. Nitrogen adsorption and desorption isotherms were measured using a Micromeritics ASAP2000 sorptometer. Sample preparation included degassing at 100 °C for 6 h. Specific surface areas and pore size distributions were calculated using the Brunauer-Emmett-Teller (BET) and Barrett-Joyner-Halenda (BJH) method, respectively. For transmission electron microscopy measurements, a small aliquot was sonicated in nanopure water for 15 min. A single drop of this suspension was placed on a lacey carbon coated copper TEM grid and dried in air. The TEM examination was completed on a Tecnai G2 F20 electron microscope.

III. Results and Discussion

The co-condensation of magnetite nanoparticles with silicate precursors in basic solution yielded the core/shell material in the presence of cetytrimethyl-ammonium bromide (CTAB) as a structure templating, and mesithylene as a pore-swelling agent. Applicability of mesithylene to induce enlargement of CTAB-templated pores was previously demonstrated [21]. The morphology and mesoporous structure of the obtained material is represented on scanning and transmission electron micrographs of WPMMSN (Fig. 1). As it can be seen from SEM image the obtained material has wide distribution of particle diameters, with the smallest particles having diameter of only 80 nm, while the biggest 750 nm. In our previous publication we noted that non-regulated agglomeration of non-functionalized iron oxide nanoparticles lead to construction of nanoparticles with wide distribution of particle diameters [19]. If phenylethyltrimethoxysilane or 3-bromopropyl-trimethoxysilane were included during the synthesis of core/shell MMSN materials more
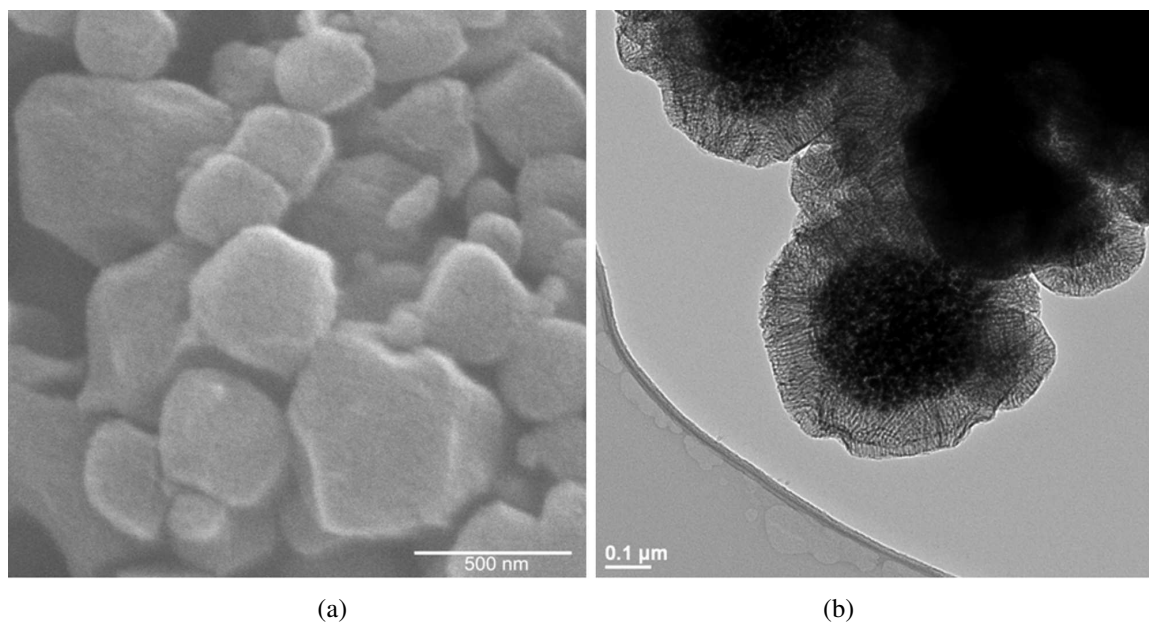

(a)   (b)

Figure 1. Electron microscopy images of WPMMSN: a) SEM and b) TEM
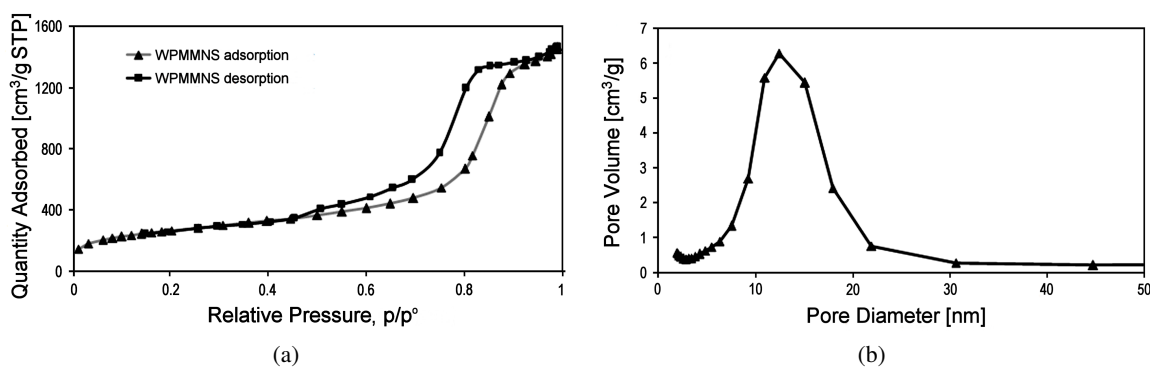

(a)   (b)

Figure 2. Low-temperature nitrogen adsorption/desorption isotherms (a) and BJH pore size distribution for WPMMSN (b)

110

evenly distributed particles were obtained, most probably due to *in situ* surface-functionalization of iron-oxide nanoparticles with the organosilanes which are thus less prone to agglomeration due to the presence of functional groups. On the TEM image (Fig. 1b), the central particle has a diameter of 600 nm, while the thickness of the mesoporous shell is 120 nm.
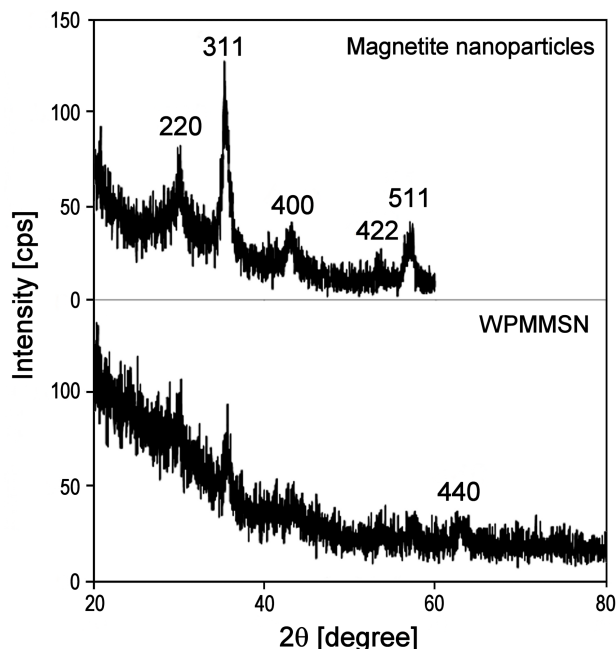

Figure 3. High-angle powder XRD of WPMMSN and magnetite nanoparticles
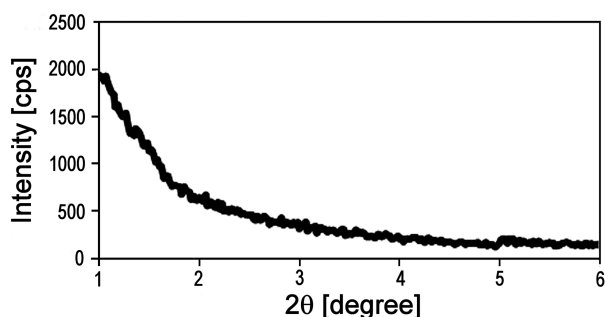

Figure 4. Low-angle powder XRD patterns of WPMMSN material

After removal of CTAB by calcination the new MMSN material showed high surface area (959 m^2/g), the average pore diameter of 12.4 nm and pore volume of 2.3 cm^3/g (Fig. 2). The measured isotherm shows a strong hysteresis loop, which is typical for bottleneck structured pores. This feature arises probably due to wide distribution of the mesopores, as it can be seen in Fig. 2b, and the pores of smaller diameter are possibly closer to the surface, while larger pores are deeper inside the particles. The high surface area and large pore diameters and volumes of WPMMSN render the material more suitable for a range of potential applications than the regular MSN and MMSN. Typical sur-

face areas of MSN and MMSN are analogous to the surface area of WPMMSN, while on the other hand, pore diameters are in the range 2–3 nm and pore volumes are around 1 cm^3/g in case of MSN and MMSN [23,24]. The bigger pores of WPMMSN would grant advantage to this material in case of some applications because of better diffusion rates of molecules, in and out of the mesopores of the material. In addition, some macromolecules, nanoparticles, proteins and other biomolecules would be capable to enter inside WP-MMSN (for potential application in drug delivery, sensing, separation etc.) but not in the materials with the smaller pores.

The XRD pattern of the as-synthesized magnetite core nanoparticles is presented in Fig. 3 and by taking the half maximum intensity width of the highest intensity peak (311) at $2\theta = 35.4°$, after accounting for instrument broadening, the calculated crystallite size from the Scherrer equation is 11.2 nm. Detailed XRD, BET, TEM and magnetic measurement analysis of a series of analogously synthesized magnetite nanoparticles can be found elsewhere [25]. Low-angle XRD measurement did not show distinctive peaks above 1 degree (Fig. 4), while high-angle exhibited the pattern of maghemite nanoparticles (Fig. 3), which is expected based on our previous observation that magnetite from the cores of core/shell materials converts to maghemite after calcination in the same conditions [19].

IV. Conclusions

Core/shell magnetic mesoporous silica nanoparticles are obtained by co-condensation of magnetite nanoparticles with silicate precursors in basic aqueous solution containing surfactant CTAB along with a pore-swelling agent mesithylene. The material exhibits high surface area, radial porous structure, wide average pore diameter and large pore volume. The material contains maghemite nanoparticles as the core, evidenced by TEM and XRD measurements, and mesoporous silica as the shell of the particles. Due to its suitable properties the prepared material may find application for drug delivery, catalysis and separation.

References

1. S. Huh, H.-T. Chen, J.W. Wiench, M. Pruski, V.S.Y. Lin, "Cooperative catalysis by general acid and base bifunctionalized mesoporous silica nanospheres", *Angew. Chem., Int. Ed.*, **44** [12] (2005) 1826–1830.
2. K. Inumaru, T. Ishihara, Y. Kamiya, T. Okuhara, S. Yamanaka, "Water-tolerant, highly active solid acid catalysts composed of the Keggin-type polyoxometalate $H_3PW_{12}O_{40}$ immobilized in hydrophobic

nanospaces of organomodified mesoporous silica", *Angew. Chem., Int. Ed.*, **46** [40] (2007) 7625–7628.

3. C. Li, H.D. Zhang, D.M. Jiang, Q.H. Yang, "Chiral catalysis in nanopores of mesoporous materials", *Chem. Commun.*, [6] (2007) 547–558.

4. M. Vallet-Regi, F. Balas, D. Arcos, "Mesoporous materials for drug delivery", *Angew. Chem., Int. Ed.*, **46** [40] (2007) 7548–7558.

5. B.G. Trewyn, I.I. Slowing, S. Giri, H.-T. Chen, V.S.Y. Lin, "Synthesis and functionalization of a mesoporous silica nanoparticle based on the sol-gel process and applications in controlled release", *Acc. Chem. Res.*, **40** [9] (2007) 846–853.

6. J. Lu, M. Liong, Z. Li, J.I. Zink, F. Tamanoi, "Biocompatibility, biodistribution, and drug-delivery efficiency of mesoporous silica nanoparticles for cancer therapy in animals", *Small*, **6** [16] (2010) 1794–1805.

7. D.R. Radu, C.-Y. Lai, J.W. Wiench, M. Pruski, V.S.Y. Lin, "Gatekeeping layer effect: A poly(lactic acid)-coated mesoporous silica nanosphere-based fluorescence probe for detection of amino-containing neurotransmitters", *J. Am. Chem. Soc.*, **126** [6] (2004) 1640–1641.

8. S. Kim, J. Ida, V.V. Guliants, J.Y.S. Lin, "Tailoring pore properties of MCM-48 silica for selective adsorption of CO_2", *J. Phys. Chem. B*, **109** [13] (2005) 6287–6293.

9. S. Oh, T. Kang, H. Kim, J. Moon, S. Hong, J. Yi, "Preparation of novel ceramic membranes modified by mesoporous silica with 3-aminopropyltriethoxysilane (APTES) and its application to Cu^{2+} separation in the aqueous phase", *J. Membrane Sci.*, **301** [1-2] (2007) 118–125.

10. R. Brady, B. Woonton, M.L. Gee, A.J. O'Connor, "Hierarchical mesoporous silica materials for separation of functional food ingredients - A review", *Innov. Food Sci. Emerg. Technol.*, **9** [2] (2008) 243–248.

11. N.Z. Knezevic, E. Ruiz-Hernandez, W.E. Hennink, M. Vallet-Regi, "Magnetic mesoporous silica-based core/shell nanoparticles for biomedical applications", *RSC Adv.*, **3** [25] (2013) 9584–9593.

12. C. Alexiou, W. Arnold, R.J. Klein, F.G. Parak, P. Hulin, C. Bergemann, W. Erhardt, S. Wagenpfeil, A.S. Lubbe, "Locoregional cancer treatment with magnetic drug targeting", *Cancer Res.*, **60** [23] (2000) 6641–6648.

13. H.X. Wu, G. Liu, S.J. Zhang, J.L. Shi, L.X. Zhang, Y. Chen, F. Chen, H.R. Chen, "Biocompatibility, MR imaging and targeted drug delivery of a rattle-type magnetic mesoporous silica nanosphere system conjugated with PEG and cancer-cell-specific ligands", *J. Mater. Chem.*, **21** [9] (2009) 3037–3045.

14. J. Kim, J.E. Lee, J. Lee, J.H. Yu, B.C. Kim, K. An, Y. Hwang, C.H. Shin, J.G. Park, J. Kim, T. Hyeon, "Magnetic fluorescent delivery vehicle using uniform mesoporous silica spheres embedded with monodisperse magnetic and semiconductor nanocrystals", *J. Am. Chem. Soc.*, **128** [3] (2006) 688–689.

15. W. Zhao, J. Shi, H. Chen, L. Zhang, "Particle size, uniformity, and mesostructure control of magnetic core/mesoporous silica shell nanocomposite spheres", *J. Mater. Res.*, **21** [12] (2006) 3080–3089.

16. Y. Deng, D. Qi, C. Deng, X. Zhang, D. Zhao, "Superparamagnetic high-magnetization microspheres with an $Fe_3O_4@SiO_2$ core and perpendicularly aligned mesoporous SiO_2 shell for removal of microcystins", *J. Am. Chem. Soc.*, **130** [1] (2008) 28–29.

17. N. Andersson, R.W. Corkery, P.C.A. Alberius, "One-pot synthesis of well ordered mesoporous magnetic carriers", *J. Mater. Chem.*, **17** [26] (2007) 2700–2705.

18. E. Ruiz-Hernandez, A. Lopez-Noriega, D. Arcos, I. Izquierdo-Barba, O. Terasaki, M. Vallet-Regi, "Aerosol-assisted synthesis of magnetic mesoporous silica spheres for drug targeting", *Chem. Mater.*, **19** [14] (2007) 3455–3463.

19. N.Z. Knezevic, I.I. Slowing, V.S.Y. Lin, "Tuning the release of anticancer drugs from magnetic iron oxide/mesoporous silica core/shell nanoparticles", *Chempluschem*, **77** [1] (2012) 48–55.

20. N.Z. Knezevic, V.S. Lin, "A magnetic mesoporous silica nanoparticle-based drug delivery system for photosensitive cooperative treatment of cancer with a mesopore-capping agent and mesopore-loaded drug", *Nanoscale*, **5** [4] (2013) 1544–1551.

21. I.I. Slowing, B.G. Trewyn, V.S.Y. Lin, "Mesoporous silica nanoparticles for intracellular delivery of membrane-impermeable proteins", *J. Am. Chem. Soc.*, **129** [28] (2007) 8845–8849.

22. L. Vayssieres, C. Chaneac, E. Tronc, J.P. Jolivet, "Size tailoring of magnetite particles formed by aqueous precipitation: An example of thermodynamic stability of nanometric oxide particles", *J. Colloid Interface Sci.*, **205** [2] (1998) 205–212.

23. M. Chen, C. Huang, C. He, W. Zhu, Y. Xu, Y. Lu, "A glucose-responsive controlled release system using glucose oxidase-gated mesoporous silica nanocontainers", *Chem. Commun.*, **48** [76] (2012) 9522–9524.

24. Y.-S. Lin, C.L. Haynes, "Synthesis and characterization of biocompatible and size-tunable multifunctional porous silica nanoparticles", *Chem. Mater.*, **21** [17] (2009) 3979–3986.

25. M. Mascolo, Y. Pei, T. Ring, "Room temperature coprecipitation synthesis of magnetite nanoparticles in a large pH window with different bases", *Materials*, **6** [12] (2013) 5549–5567.